© 2014. Published by The Company of Biologists Ltd | Development (2014) 141, 2780-2790 doi:10.1242/dev.110155

RESEARCH ARTICLE

STEM CELLS AND REGENERATION

Antagonistic regulation of p57kip2 by Hes/Hey downstream of Notch signaling and muscle regulatory factors regulates skeletal muscle growth arrest

Antoine Zalc[1,2,3,*], Shinichiro Hayashi[1,2,3,*], Frédéric Auradé[1,2,3,‡], Dominique Bröhl[4,‡], Ted Chang[1,2,3,‡], Despoina Mademtzoglou[1,2,3], Philippos Mourikis[1,2,3], Zizhen Yao[5,§], Yi Cao[5,§], Carmen Birchmeier[4] and Frédéric Relaix[1,2,3,¶]

ABSTRACT

A central question in development is to define how the equilibrium between cell proliferation and differentiation is temporally and spatially regulated during tissue formation. Here, we address how interactions between cyclin-dependent kinase inhibitors essential for myogenic growth arrest (p21^{cip1} and p57^{kip2}), the Notch pathway and myogenic regulatory factors (MRFs) orchestrate the proliferation, specification and differentiation of muscle progenitor cells. We first show that cell cycle exit and myogenic differentiation can be uncoupled. In addition, we establish that skeletal muscle progenitor cells require Notch signaling to maintain their cycling status. Using several mouse models combined with *ex vivo* studies, we demonstrate that Notch signaling is required to repress p21^{cip1} and p57^{kip2} expression in muscle progenitor cells. Finally, we identify a muscle-specific regulatory element of *p57^{kip2}* directly activated by MRFs in myoblasts but repressed by the Notch targets Hes1/Hey1 in progenitor cells. We propose a molecular mechanism whereby information provided by Hes/Hey downstream of Notch as well as MRF activities are integrated at the level of the *p57^{kip2}* enhancer to regulate the decision between progenitor cell maintenance and muscle differentiation.

KEY WORDS: Myogenesis, Cell cycle regulation, p57^{kip2}, Cdkn1, Notch signaling, MRF

INTRODUCTION

The formation of functional organs of an appropriate size is highly controlled during development. Organ transplantation and regeneration studies have revealed that organ size relies on both intrinsic and extrinsic mechanisms (reviewed by Cook and Tyers, 2007). Systemic factors, such as growth hormones and nutritional status, have been known for many years to regulate organ size, while more recently the role of the Hippo and insulin/TOR pathways has emerged (Tumaneng et al., 2012). Of note, increasing evidence links these pathways with stem cell self-renewal and differentiation (Cherrett et al., 2012). Nevertheless, how cell fate decisions and differentiation programs are coordinated with cell cycle progression and arrest remains poorly understood.

[1]UPMC Paris 06, U 974, Paris, F-75013, France. [2]INSERM, Avenir Team, Pitié-Salpétrière, Paris, F-75013, France. [3]Institut de Myologie, Paris, F-75013, France. [4]Max-Delbrück-Center for Molecular Medicine, Berlin 13125, Germany. [5]Human Biology Division, Fred Hutchinson Cancer Research Center, Seattle, WA 98109, USA.
*These authors contributed equally to this work
‡These authors contributed equally to this work
§These authors contributed equally to this work

¶Author for correspondence (frelaix@gmail.com)

Received 14 March 2014; Accepted 13 May 2014

Skeletal muscle provides a suitable model for such studies because the molecular pathways regulating differentiation and growth arrest have been identified. Muscle formation relies on a proliferating population of progenitor cells that express and require the Paired homeobox transcription factors Pax3 and Pax7 (Buckingham and Relaix, 2007). These resident progenitors are maintained in the developing muscles, where they provide a source of cells for muscle growth during development and eventually generate the adult stem cells population, termed satellite cells (Gros et al., 2005; Kassar-Duchossoy et al., 2005; Lepper and Fan, 2010; Relaix et al., 2006). Initially, muscle progenitor cells are located in the somite where they give rise to the trunk musculature of the myotome (Ben-Yair and Kalcheim, 2005; Kassar-Duchossoy et al., 2005; Relaix et al., 2005) or migrate out of the somitic dermomyotome to form limb skeletal muscles (Birchmeier and Brohmann, 2000; Schienda et al., 2006). During limb embryonic myogenesis, Pax3/7^{+} progenitor cells undergo consecutive steps of differentiation via sequential expression of bHLH myogenic regulatory factors [MRFs; Myf5, Myod1 and myogenin (Myog)], and first form committed progenitor cells that express Pax3/7 and Myf5, which correspond to a transit amplifying population (Picard and Marcelle, 2013), followed by the generation of myoblasts that express Myf5 and Myod1, culminating in the appearance of differentiating myoblasts marked by Myog (Fig. 1) (Murphy and Kardon, 2011). The Myog^{+} cells then fuse to form multinucleated muscle fibers. In the absence of Myod1, despite upregulated Myf5 expression, myogenic differentiation is delayed during early limb development, resulting in a transient absence of differentiating (Myog^{+}) myoblasts and fibers prior to E14.5 (Kablar et al., 1998). When both Myf5 and Myod1 are impaired, Pax3/7^{+} cells do not enter the myogenic program and skeletal muscle formation is abolished at all sites of myogenesis (Rudnicki et al., 1993).

Building a tissue requires the coordination of cell cycle exit with differentiation. Despite the identification of key molecular regulators of myogenic specification and differentiation (Buckingham and Relaix, 2007), how cell cycle exit is synchronized with skeletal muscle differentiation is not well understood. Cell cycle exit in muscle cells is orchestrated by cyclin-dependent kinase inhibitors (CDKIs) belonging to the CIP/Kip family: p21^{cip1} (Cdkn1a, p21^{waf1}), p27^{kip1} (Cdkn1b) and p57^{kip2} (Cdkn1c), abbreviated here as p21, p27 and p57, respectively. These CDKIs can bind and inhibit all combinations of cyclin-CDK complexes (reviewed by Besson et al., 2008). Most notably, in the absence of both *p21* and *p57*, skeletal muscle development is severely affected and fiber formation is impaired, with myogenic cells undergoing apoptosis. This points to an essential function of p21 and p57 in cell cycle arrest during myogenesis (Zhang et al., 1999). *In vitro*, Myod1 has been suggested to be a direct regulator of *p21*, thus controlling cell cycle exit during

Development (2014) 141, 2780-2790 doi:10.1242/dev.110155

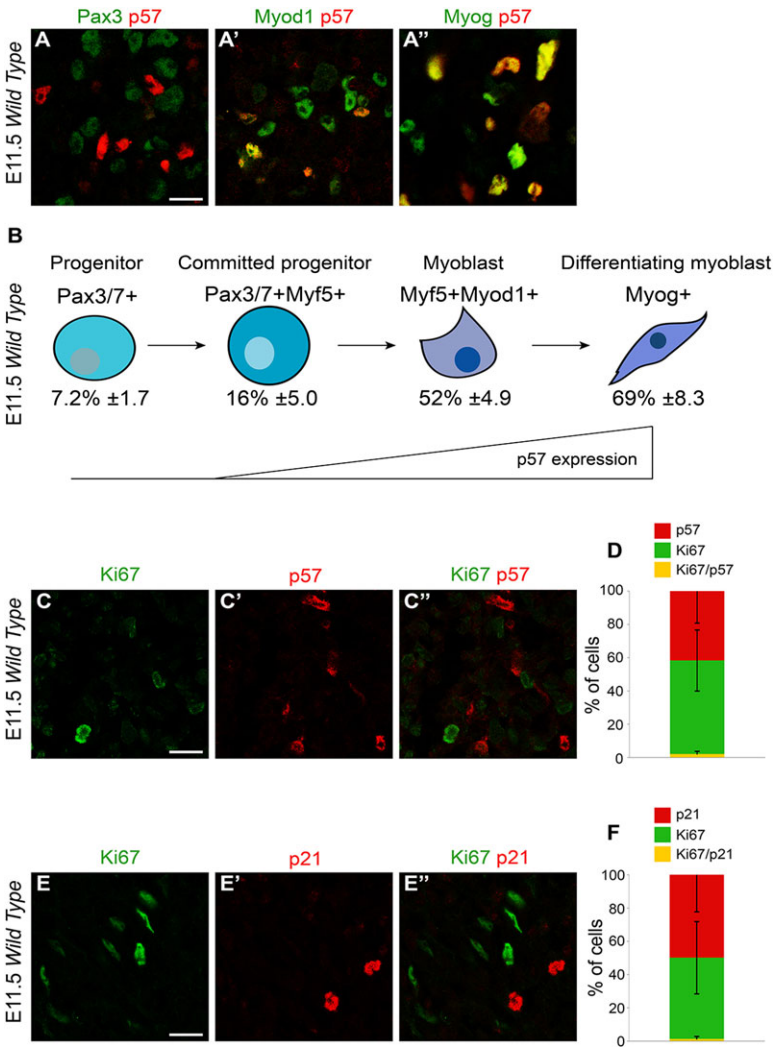

Fig. 1. Cell cycle exit occurs at the determination stage. (A-A″) Co-immunostaining for Pax3 (A), Myod1 (A′) and myogenin (Myog, A″) in green, and p57 (A′,A″) in red in E11.5 embryonic limb muscles. (B) Percentage of p57-expressing cells during forelimb myogenesis is given for each population. Progenitors and committed progenitors are mostly proliferating, whereas myoblasts and differentiating myoblasts are exiting the cell cycle. (C-C″) Co-immunostaining for Ki67 (C,C″, green) and p57 (C′,C″, red) in E11.5 embryonic limb muscles. (D) Quantification of C-C″. (E-E″) Co-immunostaining for Ki67 (E,E″, green) and p21 (E′,E″, red) in E11.5 embryonic limb muscles. (F) Quantification of E-E″. Ki67 is not expressed in cells expressing p21 or p57. For all experiments n=3 embryos; error bars indicate s.d. Scale bars: 10 μm.

adult muscle differentiation (Halevy et al., 1995). It has also been shown, both in mammalian cells (Reynaud et al., 2000) and in zebrafish (Osborn et al., 2010), that p57 interacts and stabilizes Myod1 to promote muscle differentiation, demonstrating a role for CDKIs beyond that in growth arrest. Analysis of *p21*; *p57* double-mutant mouse embryos suggested that cell cycle exit occurs in parallel to, but independently of, Myog-dependent terminal differentiation, while the lack of Mef2c expression in these mice suggested that late differentiation is defective (Zhang et al., 1999).

Previous studies have implicated the Notch signaling pathway as a key regulator of proliferation and differentiation of muscle progenitor cells (Buas and Kadesch, 2010; Mourikis and Tajbakhsh, 2014). This pathway is highly conserved during evolution and plays key roles during development, including the regulation of cell fate decisions, differentiation and homeostasis of progenitor cells in a wide variety of tissues (reviewed by Artavanis-Tsakonas and Muskavitch, 2010). Notch signaling requires direct interaction between a cell expressing at least one of the ligands [delta-like 1 (Dll1) and 4 and jagged 1 and 2 in mammals] with a cell expressing one of the receptors (notch 1-4 in mammals). This interaction leads to a proteolytic cleavage of the receptor that releases the Notch intracellular domain, which translocates into the nucleus and interacts with the Rbpj transcription factor to induce downstream effectors, such as the Hes/Hey family of bHLH transcriptional repressors (reviewed by Borggrefe and Liefke, 2012).

The role of Notch signaling in skeletal muscle development has been assessed in two mouse models: in a hypomorphic *Dll1* mutant (Schuster-Gossler et al., 2007) or in mice in which *Rbpj* expression was conditionally abrogated specifically in the myogenic lineage (Vasyutina et al., 2007). These *in vivo* models, along with studies performed in chick embryos, have demonstrated that Dll1-triggered canonical Notch signaling is required for the maintenance of muscle progenitor cells (Delfini et al., 2000; Hirsinger et al., 2001; Mourikis et al., 2012a; Schuster-Gossler et al., 2007; Vasyutina et al., 2007). Dll1 absence leads to early onset differentiation (Schuster-Gossler et al., 2007; Vasyutina et al., 2007), resulting in rapid exhaustion of the muscle progenitor cell pool and near complete absence of skeletal muscles at the fetal stage (Schuster-Gossler et al., 2007; Vasyutina et al., 2007). This is in part mediated by the repression of Myod1 target genes through direct binding of Hey1 to their promoters (Bröhl et al., 2012; Buas et al., 2010). Interestingly, the role of Notch can be context dependent, since in the young somite of the chick embryo, $Dll1^{+}$ neural crest cells provide a transient stimulation of Notch activity that is important for the initiation of early myogenesis (Rios et al., 2011).

Here, we evaluated the *in vivo* expression of p57 and its link with muscle cell differentiation. Although cell cycle exit is normally synchronous with cell differentiation, we show that these events can be uncoupled. In fact, we found that during embryonic myogenesis p57-mediated cell cycle arrest occurs earlier than

Development (2014) 141, 2780-2790 doi:10.1242/dev.110155

previously recognized, namely in determined muscle cells. Moreover, we demonstrate that in the absence of terminal differentiation muscle progenitor cells aberrantly induce p57 expression, leading to growth arrest. We further show that this growth arrest is associated with a loss of Notch signaling. This is confirmed by conditional genetic ablation of *Rbpj* that leads to upregulation of p21 and p57 in muscle progenitors associated with increased growth arrest. We finally identify a muscle-specific *p57* regulatory element and show that this enhancer is the target of both positive regulation by MRFs in myoblasts and negative regulation by Hes/Hey repressors downstream of Notch in progenitor cells. Our data therefore demonstrate that the regulation of cell cycle exit integrates both negative (via Hes/Hey downstream of Notch signaling) and positive (by MRFs) regulation at the same *p57* regulatory element during muscle differentiation, and that Notch signaling acts upstream, but independently, of both differentiation and cell growth arrest.

RESULTS

Cell cycle exit and differentiation can be uncoupled during skeletal muscle development

We first assessed whether myogenic progenitors leave the cell cycle at specific steps of the MRF-mediated differentiation program, by comparing p57 expression with that of MRFs in E11.5 mouse limbs by immunofluorescence (Fig. 1A-A″). As expected, p57 expression was very low in Pax3/7^{+} progenitors (7.2 ±1.7%). By contrast, a proportion of the Pax3/7^{+}/Myf5^{+} committed progenitor cells did express p57 (16±5%), and this proportion increased significantly in Myf5^{+}/Myod1^{+} (52±4.9%) and Myog^{+} (69±8.3%) populations (Fig. 1B). Similar results were obtained with p21 (data not shown). We verified that p21 and p57 are accurate markers of cell cycle exit of myogenic progenitors as their expression almost never co-localized with that of Ki67, a marker of cycling cells (Fig. 1C-F). Our data are consistent with the results of previous *in vivo* studies analyzing the proliferation of myogenic cells during development (Gros et al., 2005; Lagha et al., 2008; Relaix et al., 2005).

In order to test the existence of a link coupling cell cycle arrest with muscle differentiation, we first investigated whether muscle differentiation is affected when cell cycle exit is impaired. We examined whether the differentiation program proceeds normally in *p21: p57* double-null embryos, in which growth arrest is abolished (Zhang et al., 1999). In limb muscles of control mice, 4.7±1.4% of Myog-positive cells underwent proliferation as assessed by phospho-histone H3 (P-H3) (Fig. 2A-A″,C). By contrast, $p21^{-/-}$; $p57^{+/-m}$ double-mutant embryos displayed a marked increase in Myog^{+}/P-H3^{+} cells (25.2±3.2%; Fig. 2B-C). Taken together, we conclude that p21- and p57-mediated cell cycle exit and MRF-mediated myogenic differentiation can occur independently of each other.

We then examined whether the uncoupling of proliferation and differentiation that we observed in the $p21^{-/-}$; $p57^{+/-m}$ double-mutant embryos holds true in a complementary condition. Delayed myogenesis in *Myod1* mutant embryos provides a useful model for such analysis (Kablar et al., 1997). As expected, Myog and p57 co-localized in the forelimbs of control $Myod1^{+/-}$ mice at E12.5 (Fig. 2D-D″). By contrast, in the E12.5 $Myod1^{-/-}$ forelimbs, even

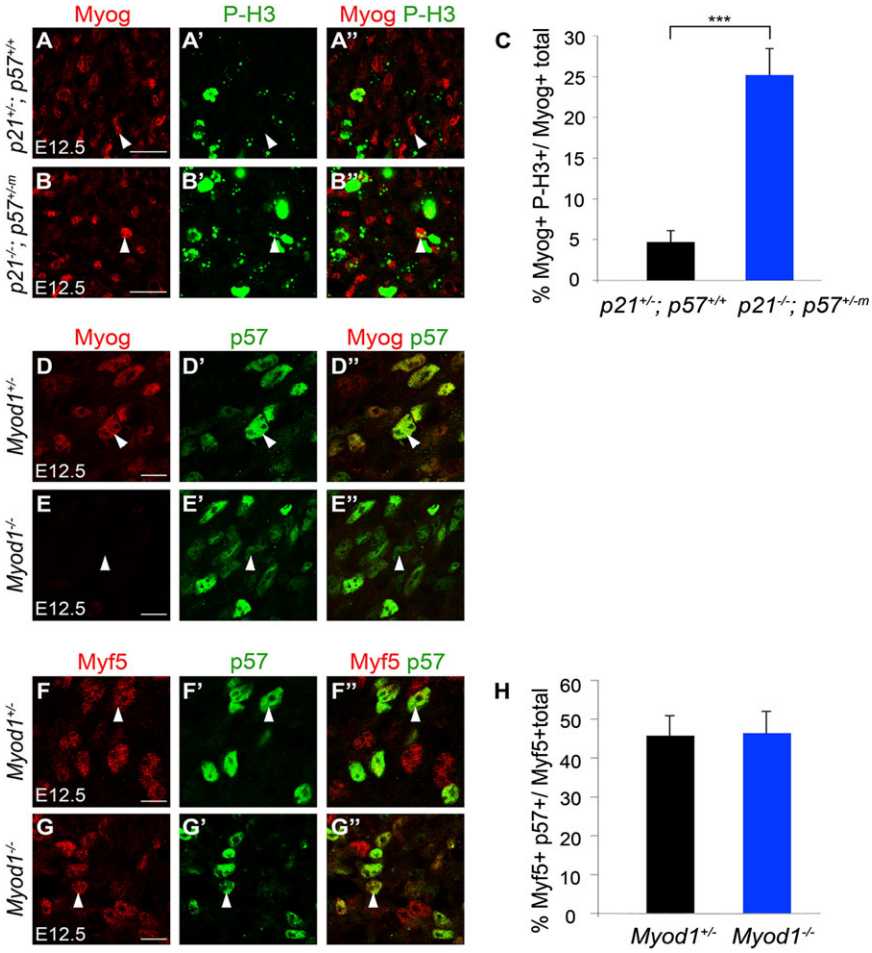

Fig. 2. Cell cycle exit can be uncoupled from cell differentiation. (A-B″) Co-immunostaining for Myog (A,A″,B,B″, red) and P-H3 (A′,A″,B′,B″, green) in $p21^{+/-}$; $p57^{+/+}$ (A-A″) or $p21^{-/-}$; $p57^{+/-m}$ (B-B″) forelimbs at E12.5. Myog^{+} cells (A) do not normally express P-H3 (A′,A″), whereas in $p21^{-/-}$; $p57^{+/-m}$ embryos Myog^{+} cells aberrantly proliferate (B-B″). (C) Quantification of A″,B″. (D-G″) Co-immunostaining for Myog (D,D″,E,E″, red), p57 (D′,D″,E′,E″,F′,F″,G′,G″, green) and Myf5 (F,F″, G,G″, red) in $Myod1^{+/-}$ (D-D″,F-F″) or $Myod1^{-/-}$ (E-E″, G-G″) embryonic limb muscles at E12.5. Myog^{+} cells express p57 in $Myod1^{+/-}$ embryos (D-D″, arrowheads). p57 is expressed in $Myod1^{-/-}$ embryos (E′) despite the absence of Myog (E). Myf5 is co-expressed with p57 in both $Myod1^{+/-}$ (F-F″, arrowheads) and $Myod1^{-/-}$ (G-G″) embryos. (H) Quantification of F″,G″. For all experiments n=3 embryos for each genotype; error bars indicate s.d.; ***P<0.001. Scale bars: 10 μm.

Development (2014) 141, 2780-2790 doi:10.1242/dev.110155

though Myog is not expressed, p57 is detected in the forming muscle masses (Fig. 2E-E″), where it labels nearly half of the Myf5^{+} cells in both *Myod1*$^{+/-}$ (Fig. 2F-F″,H) and *Myod1*$^{-/-}$ (Fig. 2G-H) forelimb (45.6±5.1% versus 46.3±5.5%). These data suggest that cell cycle exit coincides with Myf5 expression in myoblasts and is unaffected when Myod1/Myog-mediated differentiation is impaired.

In the absence of differentiated myoblasts, muscle progenitors precociously express p57 and exit the cell cycle

It has been previously shown that differentiating myoblasts are required for the survival of muscle progenitor cells throughout development (Kassar-Duchossoy et al., 2005). We examined in more detail the impact of differentiating myoblasts on the proliferation state of Pax3^{+} cells by analyzing different allelic combinations of *Myod1: Myf5* double-null embryos to allow key steps during myogenic commitment to be separated. In the absence of Myod1^{+} myoblasts but in the presence of Myf5^{+} myoblasts in *Myod1*$^{-/-}$; *Myf5*$^{+/nlacZ}$ mice (Rudnicki et al., 1993; Tajbakhsh et al., 1997) (supplementary material Fig. S1), the proliferation rate of Pax3^{+} cells was comparable to that observed in control mice at E12.5 (23.6±3.9% versus 25.6±4.6%; Fig. 3A-B″,D). By contrast, in the double-mutant *Myod1*$^{-/-}$; *Myf5*$^{nlacZ/nlacZ}$ forelimbs, which lack both committed progenitors and myoblasts (supplementary material Fig. S1), we observed a significant decrease in the proliferation of Pax3^{+} cells (12.8±3.6% versus 25.6±4.6%; Fig. 3C-D). These data suggest that committed progenitors are required to maintain the proliferation of muscle progenitor cells, whereas differentiated myoblasts are dispensable.

Consistent with the proliferation profile, the cell cycle inhibitor p57 was aberrantly expressed in Pax3^{+}/MRF^{-} progenitor cells of *Myod1*$^{-/-}$; *Myf5*$^{nlacZ/nlacZ}$ embryos compared with control embryos (28.4±2.7% versus 2.3±2.7%; Fig. 3E-G). These data suggested that myoblasts are required to maintain cycling muscle progenitor cells by preventing p57 expression and cell cycle arrest.

Impaired Notch signaling in *Myod1; Myf5* mutant embryos

Our analysis of *Myod1; Myf5* mutant embryos reinforced the notion that functional interactions are taking place between myoblasts and muscle progenitor cells. A strong candidate pathway to mediate these interactions is Notch signaling. It has been previously shown that differentiating myogenic cells express Dll1 and possibly signal to the upstream population that expresses higher levels of Notch receptors (mainly notch 1, 2 and 3) (Delfini et al., 2000; Hirsinger et al., 2001; Mourikis et al., 2012b; Schuster-Gossler et al., 2007). This feedback mechanism of receptor/ligand regulation is supported by many independent *in vivo* studies. However, it has not been formally shown that such cell-cell interactions occur during development, a prerequisite for Notch signaling.

To demonstrate an interaction between myoblasts and muscle progenitor cells, we analyzed the cellular organization on sections of embryonic forelimb muscle masses by co-immunostaining, and found that the majority of Pax7^{+} progenitor cells are in close proximity to Myod1^{+} myoblasts (Fig. 4A-B). Our analysis therefore suggests that direct cell-cell signaling via Notch can occur between progenitors and myoblasts.

To further assess the significance of differentiating muscle cells in Notch activation, we measured endogenous pathway activity in E12.5 *Myod1*; *Myf5* double-mutant embryos that lack differentiated muscle due to the MRF deficiency. It was previously shown that Pax7 expression is lost when Notch signaling is abrogated in myogenic progenitor cells (Vasyutina et al., 2007). Consistent with impaired Notch activity, Pax7 protein was undetectable by immunofluorescence at E12.5 in *Myod1*$^{-/-}$; *Myf5*$^{nlacZ/nlacZ}$ forelimbs (Fig. 4C-E), whereas it was expressed in *Myod1*$^{-/-}$; *Myf5*$^{+/nlacZ}$ embryos (Fig. 4C-E). In addition, we found downregulation of the Notch target genes *Hes1* and *Hey1* in the forelimbs of *Myod1*$^{-/-}$; *Myf5*$^{nlacZ/nlacZ}$ compared with *Myod1*$^{+/-}$; *Myf5*$^{+/nlacZ}$ or with *Myod1*$^{-/-}$; *Myf5*$^{+/nlacZ}$ at E12.5 (Fig. 4F,G).

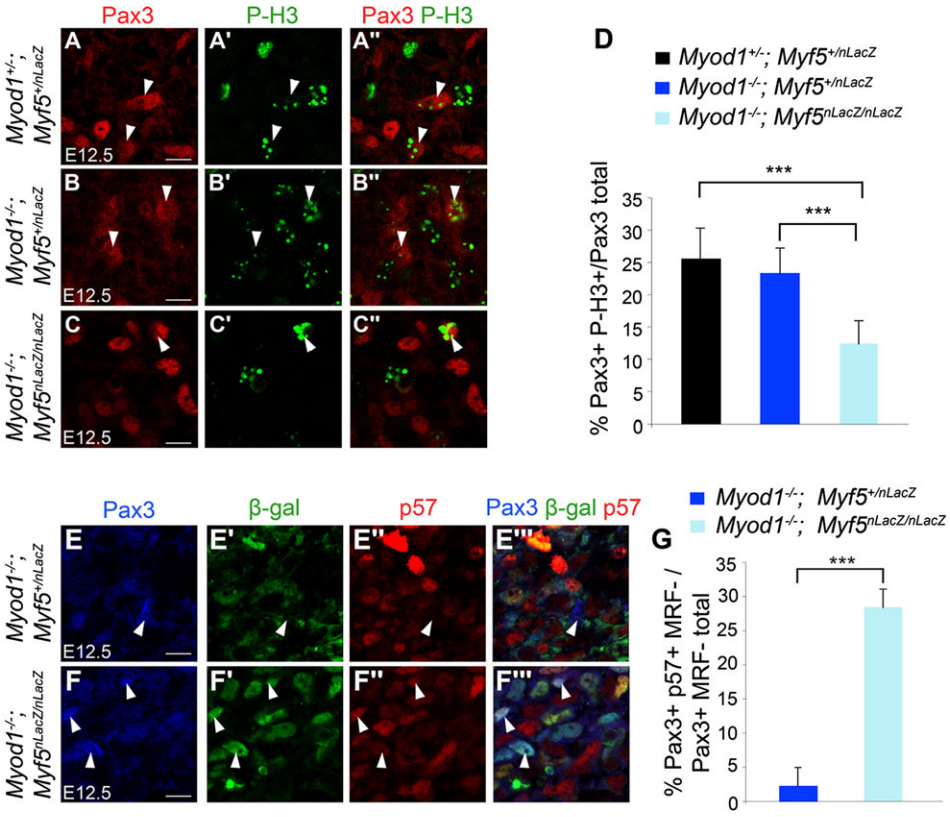

Fig. 3. Myoblasts control muscle progenitor cell proliferation by preventing cell cycle exit. (A-C″) Co-immunostaining for Pax3 (red) and P-H3 (green) in *Myod1*$^{+/-}$; *Myf5*$^{+/nlacZ}$ (A-A″), *Myod1*$^{-/-}$; *Myf5*$^{+/nlacZ}$ (B-B″) and *Myod1*$^{-/-}$; *Myf5*$^{nlacZ/nlacZ}$ (C-C″) embryos at E12.5. Arrowheads indicate Pax3^{+} cells undergoing mitosis. (D) Quantification of A″,B″,C″. (E-F‴) Co-immunostaining for Pax3 (blue), β-gal (green) and p57 (red) in *Myod1*$^{-/-}$; *Myf5*$^{+/nlacZ}$ (E-E‴) or *Myod1*$^{-/-}$; *Myf5*$^{nlacZ/nlacZ}$ (F-F‴) embryos at E12.5. Myf5^{-}/β-gal^{-} cells do not express p57 (arrowheads in E-E‴) in *Myod1*$^{-/-}$; *Myf5*$^{+/nlacZ}$ embryos, whereas in *Myod1*$^{-/-}$; *Myf5*$^{nlacZ/nlacZ}$ embryos Pax3^{+} cells are p57^{+} (arrowheads in F-F‴). (G) Quantification of E‴,F‴. For all experiments *n*=3 embryos for each genotype; error bars indicate s.d.; ***P<0.001. Scale bars: 10 μm.

Development (2014) 141, 2780-2790 doi:10.1242/dev.110155

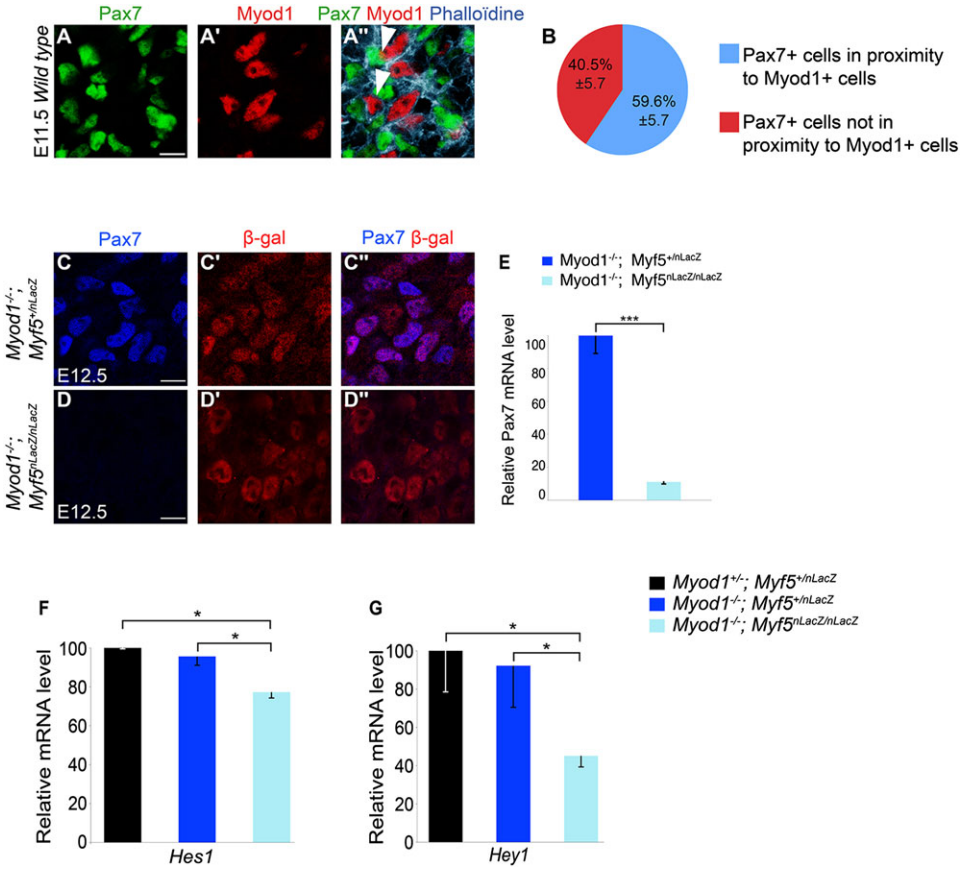

Fig. 4. Close proximity of Pax7$^+$ and Myod1$^+$ cells, with decreased Pax7 and Hes1/Hey1 expression in muscle progenitor cells of the *Myod1; Myf5* double mutant. (A-A″) Co-immunostaining for Pax7 (green) and Myod1 (red), with phalloidin (cyan) to label actin to visualize cell membranes, in wild-type limb muscles at E11.5. (B) Percentage of Pax7$^+$ cells in proximity to Myod1$^+$ cells in limb muscle masses. (C-D″) Co-immunostaining for Pax7 (blue) and β-gal (red) in *Myod1*$^{-/-}$; *Myf5*$^{+/nlacZ}$ (C-C″) and *Myod1*$^{-/-}$; *Myf5*$^{nlacZ/nlacZ}$ (D-D″) embryos at E12.5. (E-G) qRT-PCR for *Pax7* (E), *Hes1* (F) and *Hey1* (G) on E12.5 forelimbs of the genotypes indicated. For all experiments n=3 embryos for each genotype; error bars indicate s.e.m.; *P<0.05, **P<0.01, ***P<0.001. Scale bars: 10 μm.

Notch signaling prevents activation of p57 in muscle progenitor cells

Based on our results (Fig. 4) and previous reports (Georgia et al., 2006), we hypothesized that myoblasts control progenitor cell proliferation by activating the Notch/Hes1/Hey1 pathway, which would then repress p57 expression.

First, to establish whether Notch signaling participates directly in the coordinated control of cell cycle exit and differentiation, we used an *ex vivo* whole limb culture system (Zúñiga et al., 1999). We cultured E11.5 mouse forelimbs for 28 h, with or without 20 μM γ-secretase inhibitor DAPT, an inhibitor of Notch signaling. As expected, we saw decreased expression of the Notch target genes *Hes1* and *Hey1* after DAPT treatment (Fig. 5A). In addition, inhibition of Notch signaling led to reduced numbers of Pax7$^+$ cells (56.8±5.6% in control versus 27.7±7.0% in DAPT-treated limb explants; Fig. 5B′,C′,D), whereas the Myod1$^+$ cell population was increased (62.7±9.0% compared with 32.6±5.3% in control DMSO-treated explants; Fig. 5B″,C″,D), confirming previous reports (Schuster-Gossler et al., 2007; Vasyutina et al., 2007) and the robustness of our *ex vivo* model. Accordingly, we found decreased levels of *Pax7* mRNA and increased levels of *Myod1* mRNA in DAPT-treated samples (Fig. 5A). We next examined whether pharmacological inhibition of Notch signaling induces cell cycle arrest in cultured muscle progenitor cells. We found a 5-fold increase in p57 expression in Pax3$^+$/MRF$^-$ cells in DAPT-treated limb explants compared with controls (Fig. 5E-G).

To confirm these results *in vivo*, we genetically abrogated Notch signaling in progenitor cells by conditionally deleting *Rbpj*. RbpJ is a DNA-binding transcription factor and the major effector of all four Notch receptors (Fortini and Artavanis-Tsakonas, 1994; Jarriault et al., 1995; Kopan and Ilagan, 2009; Schweisguth and Posakony, 1992). We performed a conditional deletion of *Rbpj* in the Pax3 lineage by crossing *Rbpj*$^{flox/flox}$ mice (Han et al., 2002) with a *Pax3*$^{Cre/+}$ allele (Engleka et al., 2005). Ablation of *Rbpj* led to increased myogenic differentiation as previously reported (Vasyutina et al., 2007), with a severe loss of progenitor cells leading to tiny limb muscles at a fetal stage. Strikingly, both p57 and p21 were upregulated in the Pax3$^+$/Myf5$^-$ muscle progenitor cells in the forelimbs of *Rbpj*$^{flox/flox}$; *Pax3*$^{Cre/+}$ mice at E11.5, whereas Pax3 and these CDKIs were rarely co-expressed in such cells in control mice (Fig. 6A-D, see also Fig. 1). To demonstrate that expression of p21 and p57 is associated with growth arrest in these mutants, we analyzed the co-expression of Ki67 with either p57 or p21 in Pax3$^+$ muscle progenitors (Fig. 6E,F) in the forelimbs of *Rbpj*$^{flox/flox}$; *Pax3*$^{Cre/+}$ mice at E11.5. We found a small but significant increase of Pax3$^+$ cells co-expressing p21 or p57 with Ki67 in the mutant embryos; nevertheless, the large majority of the Pax3$^+$/p57$^+$ cells did not express Ki67, as predicted.

Altogether, these results demonstrate that in embryonic muscle progenitor cells Notch signaling antagonizes cell cycle exit by repressing p57 expression.

A *p57* muscle-specific enhancer is directly regulated by Notch signaling and MRFs

To gain insight into the molecular mechanisms of *p57* regulation, we used data generated by a Myod1 ChIP sequencing experiment (Cao et al., 2010) to identify Myod1 binding sites in the vicinity of the *p57* locus. A previous study had predicted that *p57* muscle-specific regulatory elements are located between +35 and +225 kb from the *p57* transcription start site (John et al., 2001). In keeping with this, a high density of Myod1 binding sites was found in a conserved region located +59 kb from *p57*. We isolated an evolutionarily conserved

Development (2014) 141, 2780-2790 doi:10.1242/dev.110155

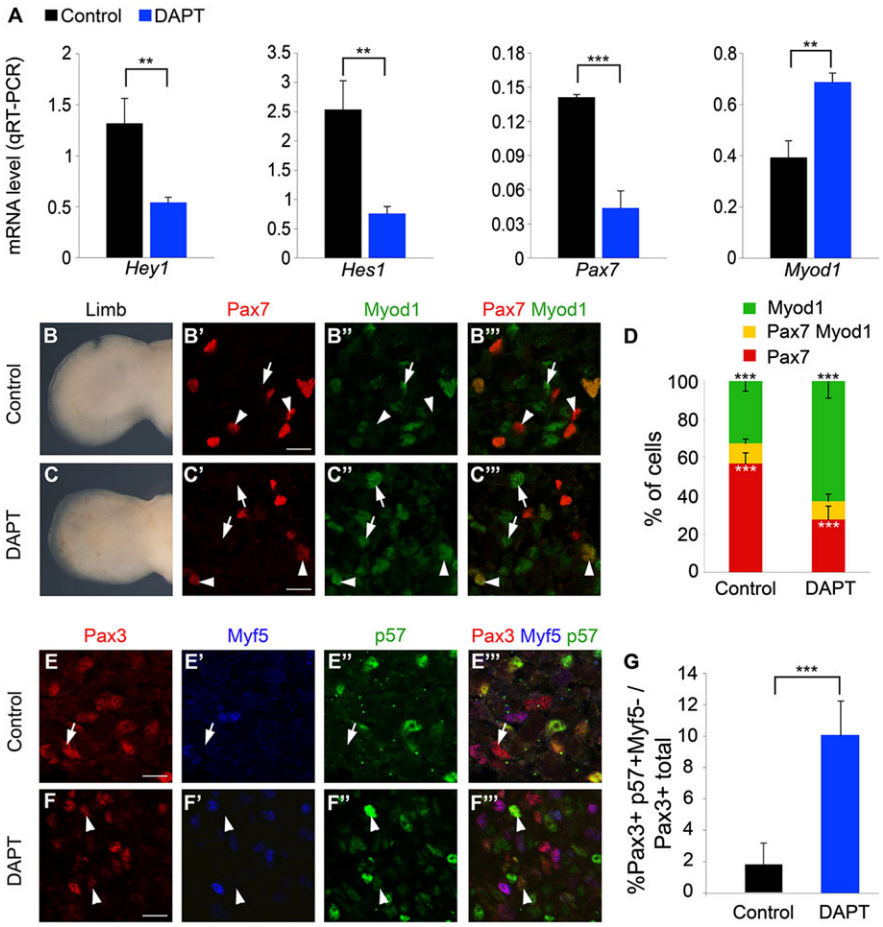

Fig. 5. The Notch pathway prevents activation of p57 in progenitor cells. (A) qRT-PCR for *Hey1*, *Hes1*, *Pax7* and *Myod1* mRNA in control (DMSO-treated) and DAPT-treated *ex vivo* whole limb culture. (B,C) An E11.5 forelimb kept in culture for 28 h treated with DMSO (B) or 20 μM DAPT (C). (B′-B‴,C′-C‴) Co-immunostaining for Pax7 (red) and Myod1 (green) in DMSO-treated (B′-B‴) or 20 μM DAPT-treated (C′-C‴) explants from E11.5 limb muscles. Arrowheads indicate Pax7^{+}/Myod1^{-} cells in B′-B‴ and Pax7^{+}/Myod1^{+} cells in C′-C‴; arrows indicate Myod1^{+}/Pax7^{-} cells. (D) Quantification of B‴,C‴. (E-F‴) Co-immunostaining for Pax3 (red), Myf5 (blue) and p57 (green) in DMSO-treated (E-E‴) or 20 μM DAPT-treated (F-F‴) explants from E11.5 limb muscles. Arrow in E-E‴ indicates a Pax3^{+}/Myf5^{-}/p57^{-} cell. Arrowheads in F-F‴ indicate Pax3^{+}/Myf5^{-}/p57^{+} cells. (G) Quantification of E‴,F‴. For all experiments n=3; error bars indicate s.d.; $^{**}P$<0.01, $^{***}P$<0.001. Scale bars: 10 μm.

686 bp fragment that contains 15 E-boxes, which are binding sites for MRFs, Hey1 and Hes1 (supplementary material Fig. S2).

We first validated this *p57* muscle regulatory element (*p57MRE*) as a functional enhancer *in vivo* by generating transgenic embryos carrying a *p57MRE-tk-nlacZ* construct. Following analysis of *lacZ* expression at E12, we detected robust reporter expression in all myogenic domains (Fig. 7A,A′), with an expression profile that matched that of Myod1. Interestingly, this element is skeletal muscle specific, since no other sites of p57 expression, such as parenchymal organs and intestine (Westbury et al., 2001), were observed. In order to characterize the myogenic cell type that expresses the p57 reporter, we performed immunohistochemical analyses on limb buds from these transgenic embryos. β-Gal^{+} cells co-expressed p57 (Fig. 7B-B″) and Myod1 (Fig. 7C-C″) but not Pax7 (Fig. 7D-D″), defining the cellular specificity of the *p57MRE*.

We next hypothesized that this regulatory element integrates negative regulation by Hes/Hey proteins and positive regulation via direct activation by the MRFs. We performed ChIP experiments on E12.5 wild-type forelimbs and found that both Myod1 and Hes1 were bound *in vivo* to the *p57MRE* fragment (Fig. 8A). To ensure that our assay was specific, and given the lack of known positive controls for Hes1 in the myogenic lineage, we performed ChIP experiments in HEK293 cells transfected with either Hes1 or Myod1 and either wild-type *p57MRE* or containing mutations in the MRF and Hes binding sites (*p57MREΔE-Boxes*). Robust binding was observed for Hes1 (Fig. 8B) and Myod1 (Fig. 8C) on the *p57MRE* and this binding was abrogated on *p57MREΔE-Boxes* (Fig. 8B,C).

Finally, to further establish this interplay between positive and negative regulation, we tested the transcriptional activity of Myod1, Hes1 and Hey1 on *p57MRE-tk-nlacZ* in transient transfection experiments in C2C12 muscle cells. Myod1 enhanced the activation of the *p57MRE* (Fig. 8D), but was not able to activate the *p57MREΔE-Boxes* element. Furthermore, Myod1 transcriptional activation was abolished when exposed to increasing concentrations of Hes1 or Hey1 (Fig. 8D), suggesting that both are able to repress the Myod1-dependent activation of *p57MRE*.

We propose a model in which the integration of Notch and MRF activities at the level of a muscle-specific enhancer of the key cell cycle arrest gene *p57* provides a means to control the equilibrium between progenitor pool amplification and the establishment of definitive functions of skeletal muscle (Fig. 8E).

DISCUSSION

The generation of organs of a defined size requires a balance between proliferation and differentiation. This balance is ensured by regulated cell growth, which prevents prolonged proliferation or premature differentiation, both of which are deleterious for normal development.

During skeletal muscle development and postnatal regeneration, Notch signaling activity is crucial for sustaining stem/progenitor cell self-renewal and its downregulation is required to allow myogenic differentiation. Cell cycle exit was previously thought to be controlled by the differentiation program (Halevy et al., 1995). In this report we show that growth arrest is also negatively regulated by Notch signaling and demonstrate that these two events, despite appearing synchronous, can be uncoupled. In *Myod1*$^{-/-}$ forelimbs, myogenesis is paused between E11.5 and E14.5 (Kablar et al., 1998). Although Myf5 is unable to drive myogenesis and activate *Myog* at these stages,

Development (2014) 141, 2780-2790 doi:10.1242/dev.110155

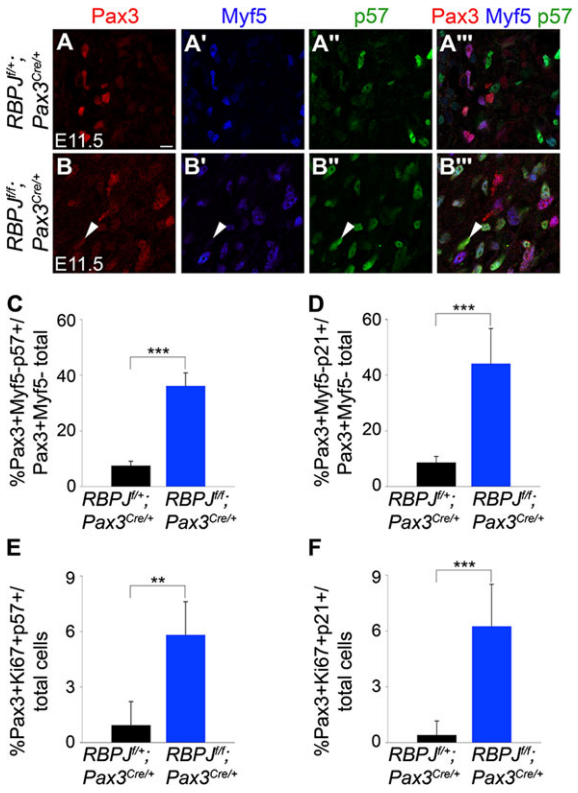

Fig. 6. Conditional ablation of *Rbpj* leads to upregulation of p57 and p21 and to cell cycle arrest in muscle progenitor cells. (A-B‴) Co-immunostaining for Pax3 (red), Myf5 (blue) or p57 (green) in $Rbpj^{flox/+}$; $Pax3^{Cre/+}$ (A-A‴) or $Rbpj^{flox/flox}$; $Pax3^{Cre/+}$ (B-B‴) forelimbs at E11.5. Arrowhead indicates a $Pax3^{+}/Myf5^{-}/p57^{+}$ cell. Scale bars: 10 μm. (C) Quantification of A‴,B‴. (D) Quantification of co-immunostaining for Pax3, Myf5 or p21 in $Rbpj^{flox/+}$; $Pax3^{Cre/+}$ or $Rbpj^{flox/flox}$; $Pax3^{Cre/+}$ forelimbs at E11.5. (E) Quantification of co-immunostaining for Pax3, Ki67 or p57 in $Rbpj^{flox/+}$; $Pax3^{Cre/+}$ or $Rbpj^{flox/flox}$; $Pax3^{Cre/+}$ forelimbs at E11.5. (F) Quantification of co-immunostaining for Pax3, Ki67 or p21 in $Rbpj^{flox/+}$; $Pax3^{Cre/+}$ or $Rbpj^{flox/flox}$; $Pax3^{Cre/+}$ forelimbs at E11.5. For all experiments n=3 embryos for each genotype; error bars indicate s.d.; $^{**}P<0.01$, $^{***}P<0.001$.

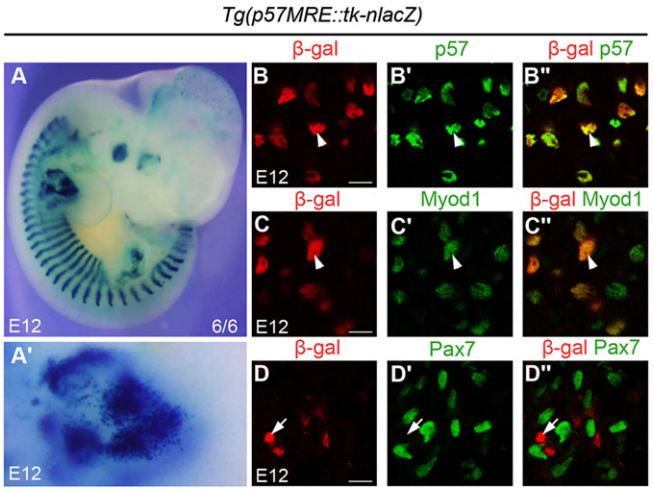

Fig. 7. Expression of a *p57* muscle regulatory enhancer (MRE) in transgenic mice. (A,A′) X-Gal staining on a transgenic *p57MRE-tk-nlacZ* embryo. A′ is a higher magnification of the forelimb region from A. (B-D″) Co-immunostaining for β-gal (B,C,D,B″,C″,D″, red), p57 (B′,B″, green), Myod1 (C′, C″, green) and Pax7 (D′,D″, green). Arrowheads indicate β-gal^{+} /p57^{+} (B-B″) and β-gal^{+}/Myod1^{+} cells (C-C″); arrows indicate β-gal^{+}/Pax7^{-} cells. Scale bars: 10 μm.

we found that $Myf5^{+}/Pax3/7^{-}$ cells expressed p57 at E12.5 and this did not prevent them from resuming differentiation at E14.5 (presumably when Mrf4 is activated). Given our finding that Myod1 directly binds and activates *p57* via the *p57MRE* sequence, we believe that Myf5 operates in the same way, thereby providing a functional uncoupling between MRF myogenic activity and growth arrest. Moreover, our study and those of others indicate that cell cycle exit occurs at the transition from committed progenitors to determined myoblasts (Fig. 1A). Consistently, we found that committed progenitor cells express Pax3/7 and Myf5, but neither p21 nor p57. This finding is consistent with the robust repressive activity exerted by Hes/Hey on MRF-mediated transactivation (Fig. 8D). The cycling status of committed progenitor cells is therefore of interest. A recent study showed that whereas the undifferentiated resident progenitor cells that express Pax7 represent a slow-cycling pool, the $Pax3/7^{+}/Myf5^{+}$ committed progenitors correspond to a fast-cycling population (Picard and Marcelle, 2013). Our study did not address the subtle cell cycle regulation of these progenitor cell populations and future studies will be required to determine whether these changes in cell proliferation are linked to Myf5 or to other, as yet unidentified, factors.

The model of coordinated regulation that we propose, with a single *p57* element integrating positive (from the MRFs) and negative (from Hes/Hey) regulatory information suggests that the interplay between Notch repression of *p57MRE* in Pax3/7 progenitors and its activation by MRFs in myoblasts is crucial for growth arrest. The molecular mechanisms regulating Notch signaling components during myogenesis are not fully characterized. It was reported that during *Xenopus* development Dll1 expression is regulated by Myod1 (Wittenberger et al., 1999) and that Myod1 expression is repressed by Hairy-1 (Umbhauer et al., 2001). It is unclear if these regulatory mechanisms also exist in amniotes, but our data are compatible with such a sequence of events. Resolving the precise molecular interplay between Pax gene expression, cell growth arrest, MRF regulation and the switch in Notch signaling will require additional investigations.

Notch signaling plays a key role in maintaining the homeostasis of muscle stem cells in the adult (Bjornson et al., 2012; Carlson et al., 2008; Fukada et al., 2011; Kitamoto and Hanaoka, 2010; Mourikis et al., 2012b) and in colonization of the satellite cell niche (Bröhl et al., 2012). In particular, Notch controls quiescence of muscle satellite cells (Bjornson et al., 2012; Mourikis et al., 2012b). This activity might be mediated by Hey1 and HeyL, which are required in the adult lineage for satellite cell homeostasis and skeletal muscle regeneration (Fukada et al., 2011). Conditional deletion of *Rbpj* in $Pax7^{+}$ satellite cells led to spontaneous differentiation without activation or division of the cells (Bjornson et al., 2012; Mourikis et al., 2012b). Strikingly, *RbpJ* ablation does not lead to an immediate and complete differentiation or growth arrest in the $Pax3^{+}$ population during embryonic development, leaving open the possibility that other pathways are involved. For instance, Notch activity on adult muscle stem cells is counteracted by TGFβ signaling (Carlson and Conboy, 2007). This is mediated through the activation of phosphorylated Smad3, which can directly bind and activate the *p15* (*Cdkn2b*), *p16* (*Cdkn2a*), *p21* and *p27* promoters (Carlson and Conboy, 2007) to favor muscle stem cell differentiation. Interestingly, during chicken myogenesis myostatin, which is a member of the TGFβ family, has also been implicated in the control of terminal differentiation through indirect activation of p21 (Manceau et al., 2008).

In addition to driving cell cycle exit during adult myogenesis, p57 has also been implicated in stabilization of Myod1 through direct association in C2C12 cells, resulting in enhanced myogenesis

Development (2014) 141, 2780-2790 doi:10.1242/dev.110155

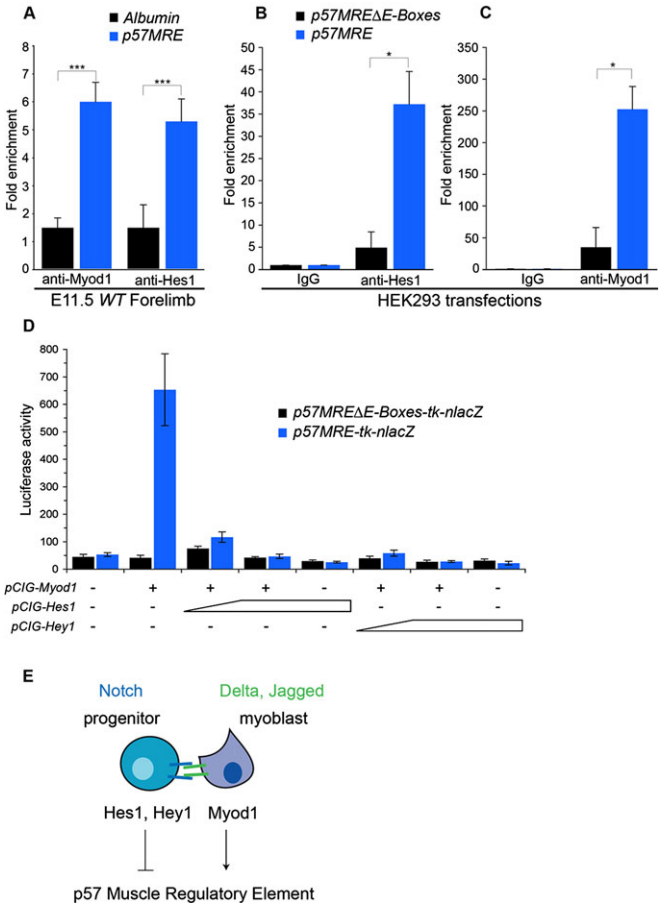

Fig. 8. Direct regulation of the *p57MRE* by Myod1 and Hes1/Hey1. (A) Chromatin immunoprecipitation followed by qPCR on wild-type forelimbs at E11.5. *p57MRE* is enriched when precipitated with anti-Myod1 or anti-Hes1 antibodies compared with an albumin gene control. (B,C) Validation of antibody ChIP capacities on transfected HEK293 cells: enrichment with anti-Hes1 (B) or anti-Myod1 (C) is obtained with the *p57MRE* compared with the construct in which all putative E-boxes have been mutated (*p57MREΔE-Boxes*). n=3; error bars indicate s.e.m.; **P*<0.05, ****P*<0.001. (D) Transactivation assay on C2C12 cells with the expression plasmids and reporters indicated ($n \geq 3$). (E) Schematic representation of the regulation of cell cycle exit during myogenesis. In muscle progenitors, Notch downstream effectors Hes1 and Hey1 repress the activation of p57 to allow the amplification of the pool, while in the neighboring myoblasts that express the Notch ligands, Myod1 directly activates p57 expression.

(Reynaud et al., 2000). A similar mechanism has also been identified in zebrafish, in which p57 cooperates with Myod1 to drive the differentiation of several early zebrafish muscle fiber types (Osborn et al., 2010). It is not known if this positive-feedback loop also operates during early murine skeletal muscle formation. One could propose that, although the initiation of myogenic differentiation and growth arrest are independent, these events may synergize subsequently, for instance to enhance Myod1 activity and reinforce terminal differentiation. In zebrafish, p57 cooperates with Myod1 to drive *myog* expression (Osborn et al., 2010); nevertheless, proliferating Myod1^{+} and Myog^{+} cells are detected in *p21*$^{-/-}$*; p57*$^{+/-}$ mice (see Fig. 2A-C; our unpublished observations). Interestingly, expression of Mef2c is impaired in these mutant mice (Zhang et al., 1999), raising the possibility that p57 may also be involved in terminal differentiation in murine myogenesis during development.

In our study, the expression of p57 is firmly linked to an absence of cell cycle progression, since we observe no overlap between p57 (or p21) expression and Ki67 (Fig. 1C-F) under normal conditions. Strikingly, a small but significant proportion of the Pax3^{+}/p21^{+} or Pax3^{+}/p57^{+} cells are Ki67^{+} in the *Pax3*$^{Cre/+}$*; Rbpj*$^{flox/flox}$ mutant context. Although this might correspond to a transitory state due to the differentiation phenotype of these mutant embryos, one cannot exclude the possibility that Notch might also be involved in both cell cycle progression and cell cycle arrest via a complex regulatory loop.

p57 expression has been reported previously in adult satellite cells (Fukada et al., 2007), but the precise timing of expression has yet to be characterized. The identification of *p57MRE* through a Myod1 ChIP-seq screen performed in C2C12 cells raises the possibility that this element is reused in adult muscle cells *in vivo*. Owing to the perinatal death of *p57* mutant mice, the role of p57 in postnatal myogenesis cannot be studied *in vivo*. *p21*-deficient mice display normal muscle development but impaired skeletal muscle regeneration (Hawke et al., 2003). Given the functional overlap between p21 and p57 during development, it would be interesting to evaluate the combined role of these two proteins in postnatal satellite cell homeostasis and skeletal muscle regeneration.

The recent identification of the role of p57 in the maintenance of quiescent hematopoietic (Matsumoto et al., 2011), neural (Furutachi et al., 2013) and lung (Zacharek et al., 2011) stem cells indicates that p57, along with other CDKIs, is important for stem cell function. Whether such a regulatory mechanism for CDKI expression is redeployed in other systems remains to be investigated. For example, Notch has been implicated in maintaining progenitor cell proliferation in intestinal stem cells (Riccio et al., 2008), in adult neural stem cells (Imayoshi et al., 2010) and in Rathke's pouch progenitors of the pituitary (Monahan et al., 2009) and, indeed, one proposed mechanism is the repression of CDKIs by the product of the Notch target gene *Hes1* (Monahan et al., 2009; Riccio et al., 2008). Unfortunately, these studies did not define which cells provide the ligands. Nevertheless, our data and the role of Notch and Hes1 in intestinal stem cells, neural stem cells and pituitary progenitor cells might suggest a general mechanism whereby the expansion of the progenitor cell population is regulated via modulation of CDKI genes. Such a regulatory mechanism could be used as a safeguard to prevent tumor formation by progenitor/stem cells, for instance when differentiation is impaired. It is also tempting to speculate that fine-tuning of this system could also be used for intrinsically regulating organ size.

MATERIALS AND METHODS

Mouse lines and harvest of embryos

Myf5$^{+/nlacZ}$, *Myod1*$^{+/-}$, *p21*$^{+/-}$, *p57*$^{+/-m}$ (*p57* is an imprinted gene; we indicate maternal origin of the allele by a superscript *m*), *Pax3*$^{Cre/+}$and *Rbpj*$^{flox/+}$ lines have been described previously (Deng et al., 1995; Engleka et al., 2005; Han et al., 2002; Rudnicki et al., 1992; Yan et al., 1997). For explant and ChIP experiments, C57BL/6J embryos were used (Janvier). For timed pregnancies, the morning when a vaginal plug was found was defined as embryonic day (E) 0.5. All experiments were performed on three independent embryos for each genotype.

Immunohistochemistry and X-Gal staining

Embryos and forelimbs were harvested and fixed for 2 h and for 20 min, respectively, in PBS/4% paraformaldehyde at 4°C. Cryoprotection was performed by equilibration in PBS/15% sucrose overnight at 4°C. Frozen sections were permeabilized in PBS/0.1% Triton X-100, blocked in PBS/2% bovine serum albumin for 1 h at room temperature, then immunolabeled with primary antibodies overnight at 4°C. For X-Gal staining, embryos were collected in PBS, fixed 20 min in PBS/4% paraformaldehyde at room temperature and incubated in X-Gal solution (Life Technologies) overnight at 37°C on a rotary shaker.

Development (2014) 141, 2780-2790 doi:10.1242/dev.110155

Antibodies

The following antibodies were used: mouse anti-β-galactosidase 1/500 (Promega, Z378), mouse anti-Myod1 5.8A 1/200 (DAKO, M3512), mouse anti-Myog F5D 1/200 (DSHB, F5D), mouse anti-p21 1/100 (BD Pharmingen, 556431), mouse anti-p57 1/100 (Santa Cruz, sc-56341), mouse anti-Pax7-c 1/100 (DSHB, Pax7-c), mouse anti-Pax3-c 1/100 (DSHB, Pax3-c), rabbit anti-β-galactosidase 1/1000 (Life Technologies, A-11132), rabbit anti-Myod1 M318 1/100 (Santa Cruz, sc-760), rabbit anti-Myf5 C20 1/500 (Santa Cruz, sc-302), rabbit anti-p57 H91 1/100 (Santa Cruz, sc-8298), rabbit anti-phospho-histone 3 Ser10 1/1000 (Cell Signaling, 9701), goat anti-p57 M20 1/50 (Santa Cruz, sc-1039) and goat anti-Pax3 1/100 (Santa Cruz, sc-34916). Phalloidin (649 nm) 1/500 was from Life Technologies. Secondary antibodies were coupled to Alexa Fluor 488 1/250, 594 1/1000 (Life Technologies) or 649 1/250 (Jackson ImmunoResearch).

Explant and cell culture

Forelimbs from E11.5 wild-type embryos were cultured in 12-well plates in BGJb medium (Life Technologies), without serum, with 200 µg/ml ascorbic acid (Sigma) and 100 µg/ml penicillin/streptomycin (Life Technologies). For Notch inhibition, forelimbs were immediately treated with 20 µM N-[N-(3,5-difluorophenacetyl)-L-alanyl]-S-phenylglycine t-butyl ester (DAPT; Sigma) or DMSO carrier (Sigma) for 28 h. Treated and control forelimbs originating from the same embryo were compared in each experiment. C2C12 and HEK293 cells were cultured in proliferating medium comprising DMEM with 10% fetal bovine serum and 100 µg/ml penicillin/streptomycin (Life Technologies).

Plasmid construct for transgenesis

The *p57* muscle regulatory element (*p57MRE*) (chr7: 150,587,238-150,587,924) was isolated by PCR. For cloning convenience, *Eag*I restriction sites were added to the forward and reverse primers used for amplification: forward, 5′-AAGCGGCCGCACCCAGTTTGCCCAGTGTAG-3′; reverse, 5′-AACGGCCGCCAGGTAAAGACACCCCAGA-3′. After *Eag*I digestion, the 686 bp fragment was cloned, respecting its genomic orientation, into the *Not*I site of p*tk*nlacZ(−) plasmid (Hadchouel et al., 2000) (*tk*, thymidine kinase). The *p57MRE-tk-nlacZ* fragment was released by *Sac*II/*Xho*I digestion and gel purified using the Nucleobond plasmid purification kit (Macherey-Nagel) before injection into pronuclei.

β-galactosidase assay

Hey1, *Hes1* cDNAs [gifts from S. Tajbakhsh (Pasteur Institute, Paris, France) and R. Kageyama (Institute for Virus Research, Kyoto University, Japan), respectively] and *Myod1* cDNA were cloned into the pCIG plasmid (Megason and McMahon, 2002). C2C12 cells were transfected with a total of 1.2 µg DNA using Lipofectamine LTX plus reagent (Life Technologies). Fixed concentrations of *p57MRE-tk-nlacZ* or *p57MREΔE-Boxes-tk-nlacZ* (0.6 µg), or pCIG-Myod1 (0.15 µg) were used. For pCIG-Hes1 and pCIG-Hey1, 0.15 or 0.3 µg was used. Each sample was co-transfected with 0.1 µg *tk*-Luciferase reporter for sample-to-sample normalization. Forty-eight hours after transfection, the cells were collected and the proteins were extracted and assayed for β-galactosidase activity (β-Gal assay Kit K1455-01, Life Technologies) and for luciferase activity (Luciferase assay system E1500, Promega) to normalize transfection variation. Measurements were made at least in triplicate and expressed as the mean (with s.e.m.) of the amount of β-galactosidase substrate (ONPG) hydrolyzed.

Reverse transcription and quantitative PCR (qPCR)

Total RNA from embryo forelimbs was extracted using the RNeasy mini kit (Qiagen). 1 µg RNA was used to generate cDNA using the Superscript II reverse transcriptase kit (Life Technologies). qPCR was performed using the Lightcycler 480 SYBR Green mix (Roche) and Lightcycler 480 II (Roche). RT-qPCR on FACS-isolated cells was performed using the Superscript III cell direct cDNA kit (Life Technologies). qPCR results are expressed as relative ratios of target cDNA to *Hprt*. The following oligonucleotides were used (5′-3′; forward and reverse): *Hes1*, ACACCGGACAAACCAAAGAC and AATGCCGGGAGCTATCTTTC; *Hey1*, CACCTGAAAATGCTGCACAC and ATGCTCAGATAACGGGCAAC; *Myod1*, GGCTACGACACCGCCTACTA and GAGATGCGCTCCACTATGCT; *Pax7*, AGGCCTTCGAGAGGACCCAC and CTGAACCAGACCTGGACGCG.

Chromatin immunoprecipitation (ChIP)

Myod1 ChIP-seq has been described in detail (Cao et al., 2010). For qPCR ChIP experiments, forelimbs from E11.5 embryos were frozen in liquid nitrogen and processed for ChIP according to the manufacturer's protocol (Active motif). 150 µg of chromatin was used for each experiment. 2 g of a rabbit anti-Myod1 M318 (Santa Cruz, sc-760) and 2 g of a goat anti-Hes1 (Santa Cruz, sc-13844) were used; 2 g of a rabbit anti-β-galactosidase (Life Technologies, A-11132) or 2 g of a goat anti-β-galactosidase (Santa Cruz, sc-19119) were used as the corresponding IgG negative control. The precipitated and input chromatins were analyzed by qPCR using *p57MRE* primers (forward, 5′-ATGTGCACACAG-CTCAGAGG-3′; reverse, 5′-GGAAGGATGGAGGGCTTTAC-3′) with albumin primers as negative control (forward, 5′-GGGACGAGATGGT-ACTTTGTG-3′; reverse, 5′-GATCAGTCCAAACTTCTTTCTG-3′).

For ChIP on transfected cells, HEK293 cells were transfected with a total of 7.5 µg DNA using FuGENE6 (Promega). A mutant *p57MRE* sequence, *p57MREΔE-Boxes*, was synthesized (GeneART) in which all putative E-boxes were mutated according to Iso et al. (2003). Fixed concentrations of *p57MRE-tk-nlacZ* or *p57MREΔE-Boxes-tk-nlacZ* (4 µg) were used together with either pCig-Myod1 or pCig-Hes1 (2 µg). After 48 h, chromatin was extracted and processed as above; 100 µg chromatin was used for each experiment. For ChIP, 2 µg normal mouse (Santa Cruz) and goat (Santa Cruz) IgG were used for negative controls for the Myod1 and Hes1 antibodies mentioned above. Results are expressed as fold change compared with IgG control.

Statistical test

Immunostainings were performed on at least three embryos of each genotype. Quantifications were performed using images of all muscle masses present in an embryo section (6-8 sections per slide, 2-3 frames per masse). All qPCR experiments were performed at least three times independently. Cell counting and qPCR results were analyzed by Mann–Whitney or Student's *t*-test. In Fig. 3D and Fig. 4F,G, quantifications were analyzed by ANOVA. In Fig. 5D, quantifications were analyzed by a chi-square test.

Acknowledgements

We are grateful to Drs Sonia Alonso-Martin, Edgar Gomes, Revital Rattenbach, Vanessa Ribes and David Sassoon for their assistance with this work and writing. We thank Catherine Bodin for histology. We also acknowledge the animal care facilities at UPMC and CDTA, and Catherine Blanc and Bénédicte Hoareau from the Flow Cytometry Core CyPS. We are grateful to Drs Tapscott and Fukada for sharing unpublished data, Drs Tajbakhsh and Kageyama for *Hey1* and *Hes1* cDNAs and F. Langa Vives for transgenic services.

Competing interests

The authors declare no competing financial interests.

Author contributions

A.Z. designed and performed experiments, analyzed data and wrote the paper. S.H. and F.A. designed and performed experiments, analyzed data and edited the manuscript. T.C., D.M. and P.M. designed and performed experiments, analyzed data. Z.Y. and Y.C. provided data on Myod1 ChIP-seq. D.B. provided *Rbpj* mutant embryos. C.B. analyzed data and edited the manuscript. F.R. oversaw the entire project, designed experiments, analyzed data and wrote the paper.

Funding

This work is supported by funding to F.R. from Institut National de la Santé et de la Recherche Médicale (INSERM) Avenir Program, Association Française contre les Myopathies (AFM), Association Institut de Myologie (AIM), Labex REVIVE, the European Union Seventh Framework Program in the project ENDOSTEM [grant # 241440], Ligue Nationale Contre le Cancer (LNCC), Association pour la Recherche contre le Cancer (ARC), Fondation pour la Recherche Médicale (FRM) [FDT20130928236], Institut National du Cancer

(INCa), Agence Nationale pour la Recherche (ANR) grant Epimuscle [grant # 11 BSV2 017 02] and Agence Nationale pour la Recherche Maladies Rares (MRAR) grant Pax3 in WS [grant # 06-MRAR-032]. This work was also funded by the German Research Foundation (DFG) [grant GK1631], French-German University (UFA-DFH) [grant CDFA-06-11] and the AFM as part of the MyoGrad International Research Training Group for Myology.

Supplementary material

Supplementary material available online at
http://dev.biologists.org/lookup/suppl/doi:10.1242/dev.110155/-/DC1

References

Artavanis-Tsakonas, S. and Muskavitch, M. A. T. (2010). Notch: the past, the present, and the future. *Curr. Top. Dev. Biol.* **92**, 1-29.

Ben-Yair, R. and Kalcheim, C. (2005). Lineage analysis of the avian dermomyotome sheet reveals the existence of single cells with both dermal and muscle progenitor fates. *Development* **132**, 689-701.

Besson, A., Dowdy, S. F. and Roberts, J. M. (2008). CDK inhibitors: cell cycle regulators and beyond. *Dev. Cell* **14**, 159-169.

Birchmeier, C. and Brohmann, H. (2000). Genes that control the development of migrating muscle precursor cells. *Curr. Opin. Cell Biol.* **12**, 725-730.

Bjornson, C. R. R., Cheung, T. H., Liu, L., Tripathi, P. V., Steeper, K. M. and Rando, T. A. (2012). Notch signaling is necessary to maintain quiescence in adult muscle stem cells. *Stem Cells* **30**, 232-242.

Borggrefe, T. and Liefke, R. (2012). Fine-tuning of the intracellular canonical Notch signaling pathway. *Cell Cycle* **11**, 264-276.

Bröhl, D., Vasyutina, E., Czajkowski, M. T., Griger, J., Rassek, C., Rahn, H.-P., Purfürst, B., Wende, H. and Birchmeier, C. (2012). Colonization of the satellite cell niche by skeletal muscle progenitor cells depends on Notch signals. *Dev. Cell* **23**, 469-481.

Buas, M. F. and Kadesch, T. (2010). Regulation of skeletal myogenesis by Notch. *Exp. Cell Res.* **316**, 3028-3033.

Buas, M. F., Kabak, S. and Kadesch, T. (2010). The Notch effector Hey1 associates with myogenic target genes to repress myogenesis. *J. Biol. Chem.* **285**, 1249-1258.

Buckingham, M. and Relaix, F. (2007). The role of Pax genes in the development of tissues and organs: Pax3 and Pax7 regulate muscle progenitor cell functions. *Annu. Rev. Cell Dev. Biol.* **23**, 645-673.

Cao, Y., Yao, Z., Sarkar, D., Lawrence, M., Sanchez, G. J., Parker, M. H., MacQuarrie, K. L., Davison, J., Morgan, M. T., Ruzzo, W. L. et al. (2010). Genome-wide MyoD binding in skeletal muscle cells: a potential for broad cellular reprogramming. *Dev. Cell* **18**, 662-674.

Carlson, M. E. and Conboy, I. M. (2007). Regulating the Notch pathway in embryonic, adult and old stem cells. *Curr. Opin. Pharmacol.* **7**, 303-309.

Carlson, M. E., Hsu, M. and Conboy, I. M. (2008). Imbalance between pSmad3 and Notch induces CDK inhibitors in old muscle stem cells. *Nature* **454**, 528-532.

Cherrett, C., Furutani-Seiki, M. and Bagby, S. (2012). The Hippo pathway: key interaction and catalytic domains in organ growth control, stem cell self-renewal and tissue regeneration. *Essays Biochem.* **53**, 111-127.

Cook, M. and Tyers, M. (2007). Size control goes global. *Curr. Opin. Biotechnol.* **18**, 341-350.

Delfini, M. C., Hirsinger, E., Pourquie, O. and Duprez, D. (2000). Delta 1-activated notch inhibits muscle differentiation without affecting Myf5 and Pax3 expression in chick limb myogenesis. *Development* **127**, 5213-5224.

Deng, C., Zhang, P., Harper, J. W., Elledge, S. J. and Leder, P. (1995). Mice lacking p21CIP1/WAF1 undergo normal development, but are defective in G1 checkpoint control. *Cell* **82**, 675-684.

Engleka, K. A., Gitler, A. D., Zhang, M., Zhou, D. D., High, F. A. and Epstein, J. A. (2005). Insertion of Cre into the Pax3 locus creates a new allele of Splotch and identifies unexpected Pax3 derivatives. *Dev. Biol.* **280**, 396-406.

Fortini, M. E. and Artavanis-Tsakonas, S. (1994). The suppressor of hairless protein participates in notch receptor signaling. *Cell* **79**, 273-282.

Fukada, S.-i., Uezumi, A., Ikemoto, M., Masuda, S., Segawa, M., Tanimura, N., Yamamoto, H., Miyagoe-Suzuki, Y. and Takeda, S. (2007). Molecular signature of quiescent satellite cells in adult skeletal muscle. *Stem Cells* **25**, 2448-2459.

Fukada, S.-i., Yamaguchi, M., Kokubo, H., Ogawa, R., Uezumi, A., Yoneda, T., Matev, M. M., Motohashi, N., Ito, T., Zolkiewska, A. et al. (2011). Hesr1 and Hesr3 are essential to generate undifferentiated quiescent satellite cells and to maintain satellite cell numbers. *Development* **138**, 4609-4619.

Furutachi, S., Matsumoto, A., Nakayama, K. I. and Gotoh, Y. (2013). p57 controls adult neural stem cell quiescence and modulates the pace of lifelong neurogenesis. *EMBO J.* **32**, 970-981.

Georgia, S., Soliz, R., Li, M., Zhang, P. and Bhushan, A. (2006). p57 and Hes1 coordinate cell cycle exit with self-renewal of pancreatic progenitors. *Dev. Biol.* **298**, 22-31.

Gros, J., Manceau, M., Thomé, V. and Marcelle, C. (2005). A common somitic origin for embryonic muscle progenitors and satellite cells. *Nature* **435**, 954-958.

Hadchouel, J., Tajbakhsh, S., Primig, M., Chang, T. H., Daubas, P., Rocancourt, D. and Buckingham, M. (2000). Modular long-range regulation of Myf5 reveals unexpected heterogeneity between skeletal muscles in the mouse embryo. *Development* **127**, 4455-4467.

Halevy, O., Novitch, B. G., Spicer, D. B., Skapek, S. X., Rhee, J., Hannon, G. J., Beach, D. and Lassar, A. B. (1995). Correlation of terminal cell cycle arrest of skeletal muscle with induction of p21 by MyoD. *Science* **267**, 1018-1021.

Han, H., Tanigaki, K., Yamamoto, N., Kuroda, K., Yoshimoto, M., Nakahata, T., Ikuta, K. and Honjo, T. (2002). Inducible gene knockout of transcription factor recombination signal binding protein-J reveals its essential role in T versus B lineage decision. *Int. Immunol.* **14**, 637-645.

Hawke, T. J., Meeson, A. P., Jiang, N., Graham, S., Hutcheson, K., DiMaio, J. M. and Garry, D. J. (2003). p21 is essential for normal myogenic progenitor cell function in regenerating skeletal muscle. *Am. J. Physiol. Cell Physiol.* **285**, C1019-C1027.

Hirsinger, E., Malapert, P., Dubrulle, J., Delfini, M. C., Duprez, D., Henrique, D., Ish-Horowicz, D. and Pourquie, O. (2001). Notch signalling acts in postmitotic avian myogenic cells to control MyoD activation. *Development* **128**, 107-116.

Imayoshi, I., Sakamoto, M., Yamaguchi, M., Mori, K. and Kageyama, R. (2010). Essential roles of Notch signaling in maintenance of neural stem cells in developing and adult brains. *J. Neurosci.* **30**, 3489-3498.

Iso, T., Kedes, L. and Hamamori, Y. (2003). HES and HERP families: multiple effectors of the Notch signaling pathway. *J. Cell Physiol.* **194**, 237-255.

Jarriault, S., Brou, C., Logeat, F., Schroeter, E. H., Kopan, R. and Israel, A. (1995). Signalling downstream of activated mammalian Notch. *Nature* **377**, 355-358.

John, R. M., Ainscough, J. F.-X., Barton, S. C. and Surani, M. A. (2001). Distant cis-elements regulate imprinted expression of the mouse p57(Kip2) (Cdkn1c) gene: implications for the human disorder, Beckwith–Wiedemann syndrome. *Hum. Mol. Genet.* **10**, 1601-1609.

Kablar, B., Krastel, K., Ying, C., Asakura, A., Tapscott, S. J. and Rudnicki, M. A. (1997). MyoD and Myf-5 differentially regulate the development of limb versus trunk skeletal muscle. *Development* **124**, 4729-4738.

Kablar, B., Asakura, A., Krastel, K., Ying, C., May, L. L., Goldhamer, D. J. and Rudnicki, M. A. (1998). MyoD and Myf-5 define the specification of musculature of distinct embryonic origin. *Biochem. Cell Biol.* **76**, 1079-1091.

Kassar-Duchossoy, L., Giacone, E., Gayraud-Morel, B., Jory, A., Gomès, D. and Tajbakhsh, S. (2005). Pax3/Pax7 mark a novel population of primitive myogenic cells during development. *Genes Dev.* **19**, 1426-1431.

Kitamoto, T. and Hanaoka, K. (2010). Notch3 null mutation in mice causes muscle hyperplasia by repetitive muscle regeneration. *Stem Cells* **28**, 2205-2216.

Kopan, R. and Ilagan, M. X. G. (2009). The canonical Notch signaling pathway: unfolding the activation mechanism. *Cell* **137**, 216-233.

Lagha, M., Kormish, J. D., Rocancourt, D., Manceau, M., Epstein, J. A., Zaret, K. S., Relaix, F. and Buckingham, M. E. (2008). Pax3 regulation of FGF signaling affects the progression of embryonic progenitor cells into the myogenic program. *Genes Dev.* **22**, 1828-1837.

Lepper, C. and Fan, C.-M. (2010). Inducible lineage tracing of Pax7-descendant cells reveals embryonic origin of adult satellite cells. *Genesis* **48**, 424-436.

Manceau, M., Gros, J., Savage, K., Thome, V., McPherron, A., Paterson, B. and Marcelle, C. (2008). Myostatin promotes the terminal differentiation of embryonic muscle progenitors. *Genes Dev.* **22**, 668-681.

Matsumoto, A., Takeishi, S., Kanie, T., Susaki, E., Onoyama, I., Tateishi, Y., Nakayama, K. and Nakayama, K. I. (2011). p57 is required for quiescence and maintenance of adult hematopoietic stem cells. *Cell Stem Cell* **9**, 262-271.

Megason, S. and McMahon, A. (2002). A mitogen gradient of dorsal midline Wnts organizes growth in the CNS. *Development* **129**, 2087-2098.

Monahan, P., Rybak, S. and Raetzman, L. T. (2009). The notch target gene HES1 regulates cell cycle inhibitor expression in the developing pituitary. *Endocrinology* **150**, 4386-4394.

Mourikis, P. and Tajbakhsh, S. (2014). Distinct contextual roles for Notch signalling in skeletal muscle stem cells. *BMC Dev. Biol.* **14**, 2.

Mourikis, P., Gopalakrishnan, S., Sambasivan, R. and Tajbakhsh, S. (2012a). Cell-autonomous Notch activity maintains the temporal specification potential of skeletal muscle stem cells. *Development* **139**, 4536-4548.

Mourikis, P., Sambasivan, R., Castel, D., Rocheteau, P., Bizzarro, V. and Tajbakhsh, S. (2012b). A critical requirement for notch signaling in maintenance of the quiescent skeletal muscle stem cell state. *Stem Cells* **30**, 243-252.

Murphy, M. and Kardon, G. (2011). Origin of vertebrate limb muscle: the role of progenitor and myoblast populations. *Curr. Top. Dev. Biol.* **96**, 1-32.

Osborn, D. P. S., Li, K., Hinits, Y. and Hughes, S. M. (2010). Cdkn1c drives muscle differentiation through a positive feedback loop with Myod. *Dev. Biol.* **350**, 464-475.

Picard, C. A. and Marcelle, C. (2013). Two distinct muscle progenitor populations coexist throughout amniote development. *Dev. Biol.* **373**, 141-148.

Relaix, F., Rocancourt, D., Mansouri, A. and Buckingham, M. (2005). A Pax3/Pax7-dependent population of skeletal muscle progenitor cells. *Nature* **435**, 948-953.

Development (2014) 141, 2780-2790 doi:10.1242/dev.110155

Relaix, F., Montarras, D., Zaffran, S., Gayraud-Morel, B., Rocancourt, D., Tajbakhsh, S., Mansouri, A., Cumano, A. and Buckingham, M. (2006). Pax3 and Pax7 have distinct and overlapping functions in adult muscle progenitor cells. *J. Cell Biol.* **172**, 91-102.

Reynaud, E. G., Leibovitch, M. P., Tintignac, L. A. J., Pelpel, K., Guillier, M. and Leibovitch, S. A. (2000). Stabilization of MyoD by direct binding to p57(Kip2). *J. Biol. Chem.* **275**, 18767-18776.

Riccio, O., van Gijn, M. E., Bezdek, A. C., Pellegrinet, L., van Es, J. H., Zimber-Strobl, U., Strobl, L. J., Honjo, T., Clevers, H. and Radtke, F. (2008). Loss of intestinal crypt progenitor cells owing to inactivation of both Notch1 and Notch2 is accompanied by derepression of CDK inhibitors p27Kip1 and p57Kip2. *EMBO Rep.* **9**, 377-383.

Rios, A. C., Serralbo, O., Salgado, D. and Marcelle, C. (2011). Neural crest regulates myogenesis through the transient activation of NOTCH. *Nature* **473**, 532-535.

Rudnicki, M. A., Braun, T., Hinuma, S. and Jaenisch, R. (1992). Inactivation of MyoD in mice leads to up-regulation of the myogenic HLH gene Myf-5 and results in apparently normal muscle development. *Cell* **71**, 383-390.

Rudnicki, M. A., Schnegelsberg, P. N. J., Stead, R. H., Braun, T., Arnold, H.-H. and Jaenisch, R. (1993). MyoD or Myf-5 is required for the formation of skeletal muscle. *Cell* **75**, 1351-1359.

Schienda, J., Engleka, K. A., Jun, S., Hansen, M. S., Epstein, J. A., Tabin, C. J., Kunkel, L. M. and Kardon, G. (2006). Somitic origin of limb muscle satellite and side population cells. *Proc. Natl. Acad. Sci. U.S.A.* **103**, 945-950.

Schuster-Gossler, K., Cordes, R. and Gossler, A. (2007). Premature myogenic differentiation and depletion of progenitor cells cause severe muscle hypotrophy in Delta1 mutants. *Proc. Natl. Acad. Sci. U.S.A.* **104**, 537-542.

Schweisguth, F. and Posakony, J. W. (1992). Suppressor of Hairless, the Drosophila homolog of the mouse recombination signal-binding protein gene, controls sensory organ cell fates. *Cell* **69**, 1199-1212.

Tajbakhsh, S., Rocancourt, D., Cossu, G. and Buckingham, M. (1997). Redefining the genetic hierarchies controlling skeletal myogenesis: Pax-3 and Myf-5 act upstream of MyoD. *Cell* **89**, 127-138.

Tumaneng, K., Russell, R. C. and Guan, K.-L. (2012). Organ size control by Hippo and TOR pathways. *Curr. Biol.* **22**, R368-R379.

Umbhauer, M., Boucaut, J.-C. and Shi, D.-L. (2001). Repression of XMyoD expression and myogenesis by Xhairy-1 in Xenopus early embryo. *Mech. Dev.* **109**, 61-68.

Vasyutina, E., Lenhard, D. C., Wende, H., Erdmann, B., Epstein, J. A. and Birchmeier, C. (2007). RBP-J (Rbpsuh) is essential to maintain muscle progenitor cells and to generate satellite cells. *Proc. Natl. Acad. Sci. U.S.A.* **104**, 4443-4448.

Westbury, J., Watkins, M., Ferguson-Smith, A. C. and Smith, J. (2001). Dynamic temporal and spatial regulation of the cdk inhibitor p57(kip2) during embryo morphogenesis. *Mech. Dev.* **109**, 83-89.

Wittenberger, T., Steinbach, O. C., Authaler, A., Kopan, R. and Rupp, R. A. W. (1999). MyoD stimulates delta-1 transcription and triggers notch signaling in the Xenopus gastrula. *EMBO J.* **18**, 1915-1922.

Yan, Y., Frisen, J., Lee, M. H., Massague, J. and Barbacid, M. (1997). Ablation of the CDK inhibitor p57Kip2 results in increased apoptosis and delayed differentiation during mouse development. *Genes Dev.* **11**, 973-983.

Zacharek, S. J., Fillmore, C. M., Lau, A. N., Gludish, D. W., Chou, A., Ho, J. W., Zamponi, R., Gazit, R., Bock, C., Jäger, N. et al. (2011). Lung stem cell self-renewal relies on BMI1-dependent control of expression at imprinted loci. *Cell Stem Cell* **9**, 272-281.

Zhang, P., Wong, C., Liu, D., Finegold, M., Harper, J. W. and Elledge, S. J. (1999). p21(CIP1) and p57(KIP2) control muscle differentiation at the myogenin step. *Genes Dev.* **13**, 213-224.

Zúñiga, A., Haramis, A.-P. G., McMahon, A. P. and Zeller, R. (1999). Signal relay by BMP antagonism controls the SHH/FGF4 feedback loop in vertebrate limb buds. *Nature* **401**, 598-602.